J. S. Afr. Inst. Min. Metall., vol. 87, no. 4.
Apr. 1987. pp. 93-106.

The growth of fatigue cracks in rail steel

by J.H. BULLOCH*

SYNOPSIS

A study of fatigue-crack growth in a rail steel and an associated weld metal showed that fatigue cracks in the deformed rail steel had slightly higher growth rates than in undeformed rail steel. The crack growth in the weld metal was appreciably faster than either and exhibited plateaux that were above the upper bound reported for rail steels.

The cyclic-life curves showed that, over an indicated service period of 8 years, both the deformed and the undeformed rail steels should not be prone to fatigue failures under the defined mechanical conditions. For the weld metal, the cyclic-life curves indicated the possibility of premature fatigue failures but, as all the input parameters represented a 'worst case' situation, this assessment could well be ultra-conservative.

In the rail steels at low ΔK levels, the extension of the fatigue cracks occurred by ductile striated growth. At a K_{max} level of 35 MPa $\sqrt{m}$, cleavage facets formed initially on the surface of the fatigue fractures, and their incidence increased with K_{max} until the onset of fast failure. The microstructure of the deformed rail steel exhibited cleavage facets at a slightly lower K_{max} value, and contained more cleavage facets at a given K level, than the microstructure of the undeformed rail steel. The average size of the cleavage facets agreed well with the pearlite nodule dimensions of 60 to 100 μm.

The microstructure of the weld metal was much coarser and contained columnar grains. At all ΔK levels, the dominant fracture mode was cleavage, with small isolated regions of ductile striated fatigue cracks. The size of the cleavage facets varied from 150 to 600 μm, and such a variation may be explained by the fact that cracking generally occurs in association with the pro-eutectoid ferrite phase, and that this phase is distributed along some boundaries of prior austenite grains and the boundaries of the coarser columnar grains.

SAMEVATTING

'n Studie van die groei van vermoeidheidskrake in spoorstaafstaal en 'n geassosieerde sweismetaal het getoon dat die groeitempo van vermoeidheidskrake in die vervormde spoorstaafstaal effens hoër is as in onvervormde spoorstaafstaal. Die groei van vermoeidheidskrake in die sweismetaal was aanmerklik vinniger as in die vervormde of onvervormde spoorstaafstaal en het plato's getoon wat bokant die boonste grens vir spoorstaafstaal is.

Die siklus-lewensduurkrommes het getoon dat sowel die vervormde as onvervormde spoorstaafstaal oor 'n aangeduide dienstyd van 8 jaar onder die omskrewe meganiese toestande nie aan vermoeidheidsfaling onderhewig behoort te wees nie. Vir die sweismetaal het die siklus-lewensduurkrommes op 'n moontlikheid van vroeë vermoeidheidsfaling gedui, maar aangesien al die toevoerparameters 'n situasie van die ergste geval verteenwoordig het, kan hierdie valuering moontlik ultrakonserwatief wees.

In die spoorstaafstaal met 'n lae ΔK-peil, het die verlenging van die vermoeidskrake plaasgevind deur gestreepte rekgroei. By 'n K_{maks}-peil van 35 MPA $\sqrt{m}$ het daar aanvanklik splytfasette op die oppervlak van die vermoeidheidsbreuke gevorm en hul voorkoms het met die K_{maks} toegeneem tot die aanvang van vinnige faling. Die mikrostruktuur van die vervormde spoorstaafstaal het splytfasette by 'n effens laer K_{maks} getoon en meer splytfasette by 'n gegewe K-peil gehad as die mikrostruktuur van die onvervormde spoorstaafstaal. Die gemiddelde grootte van die splytfasette het goed ooreengekom met die afmetings van perlietnodule van 60 tot 100 μm.

Die mikrostruktuur van die sweismetaal was baie growwer en het kolomvormige korrels ingesluit. Splyting was by alle ΔK-peile die oorheersende breukwyse, met klein geïsoleerde plekke met gestreepte rekvermoeidheidskrake. Die grootte van die splytfasette het van 150 tot 600 μm gewissel en sodanige variasie kan verklaar word deur die feit dat kraking oor die algemeen plaasvind in assosiasie met die pro-eutektoïedferrietfase en dat hierdie fase versprei is langs sommige grense van vroeëre oustenietkorrels en die grense van die growwer kolomvormige korrels.

Introduction

A recent preliminary assessment[1] of the fatigue life of rail steels indicated that, during normal operation, failures as a result of the growth of fatigue cracks can be expected within 5 to 10 years in rails that contain an initial surface defect of 2 mm.

It was found that, shortly after rails had been laid, local substantial deflection of the sleepers occurred as a result of regions of weak support in the ballast, causing the rails to undergo permanent plastic deformation. As a result of this, it was thought pertinent to study the effect of imposed plastic deformation on the growth of fatigue cracks in rail steels and to attempt a more rigorous assessment of the safety life of rails.

Part 1 of the present paper describes fatigue-crack growth in deformed (ϵ = 0,1 per cent) and undeformed rail steel and associated weld metal. In the study, an approach involving linear elastic fracture mechanics (L.E.F.M.) was used, and cyclic-life characteristics were determined, which illustrate the usefulness and predictive capabilities of such an approach. Part 2 gives a full metallographic and fractographic assessment of the same test specimens.

PART 1: ASSESSMENT OF CYCLIC LIFE

Two rail sections, one deformed and one undeformed, and a region of weld metal were supplied to the University of the Witwatersrand. From each material, the following mechanical test specimens were machined:

(a) a single-edge notch pin-loaded tensile specimen, with a width of 37 mm and a thickness of 5 mm, and

* Senior Research Officer, Department of Metallurgy, University of the Witwatersrand, 1 Jan Smuts Avenue, Johannesburg 2001.

 Paper received 10th December, 1985. SA ISSN 0038-223X/$3.00 + 0.00.

(b) an hour-glass stress/cycle test specimen, with a diameter of 5 mm, a gauge length of 20 mm, and a final machined surface.

Two Houndsfield tensile specimens of 5 mm diameter and 20 mm in length were machined from the undeformed rail so that the tensile properties could be assessed. Also, a section of undeformed rail was plastically deformed in the laboratory by $\epsilon = 0,1$ per cent, the calculated service deformation. Both the stress/cycle specimen ('in service' steel) and the fatigue-crack specimens were machined from the laboratory-deformed rail steel so that their fatigue characteristics could be compared.

Determinations of fatigue-crack growth were carried out in air on a 50 kN servo-hydraulic test facility, with an R-ratio of about 0,1, under a sine waveform at a frequency of 30 Hz.

Limited stress/cycle tests were conducted to simulate the number of cycles at a particular stress range that the rails would experience during a service life of 8 years[2]. In this particular study, the two maximum levels of stress ($\Delta\sigma$) were considered relevant to the problem: 16 000 cycles at $\Delta\sigma = 155$ MPa and 448 000 cycles at $\Delta\sigma = 104$ MPa. The test frequency was 30 Hz, and the R-ratio 0,1.

Experimental Results

Duplicate tensile tests on the undeformed rail steel exhibited good agreement with 0,2 per cent proof stress = 475 MPa and ultimate tensile strength (U.T.S.) = 955 MPa.

No failures occurred during the testing of the stress/cycle specimens, indicating that, under the stress ranges and number of cycles associated with 8 years' service, crack initiation in undefective rail steels and weld metal should not occur. This is in agreement with the work of Hill and Bootle[3], who have shown that the fatigue limit ($\Delta\sigma_w$) of rail steels and selected structural steels approaches 200 MPa. The results for fatigue-crack growth are shown in Fig. 1. It can be seen that those for the underformed rail lie midway between the upper and lower bounds for rail steels taken from a detailed survey of crack growth in such steels in the U.S.A.[4].

The results for the 'in service' and laboratory-deformed rail steel, which show good agreement and lie towards the upper bound, exhibited growth that is consistently 2 to 3 times faster than that in the undeformed rail steel.

The results for fatigue-crack growth in the weld metal did not show the usual Paris Law straight-line dependence with ΔK. In this case, the crack growth appeared to be locally unstable and exhibited plateaux that in some cases were 5 times faster than the upper bound for rail steels. For analysis purposes, a straight line in common with the Paris Law was constructed through the peaks of the plateaux.

With the exception of the weld metal, the growth of fatigue cracks in the rail steel materials tested in the present investigation was within the upper bound given by Steele[4]. Paris Law equations for the data shown in Fig. 1 are listed in Table I.

An optical investigation was conducted on the fatigue-crack fracture surfaces of each specimen. The rail steels exhibited sub-critical transgranular cleavage failure, the incidence of which increased with increasing K_{max} (ΔK). The deformed rail steels exhibited more of these cleavage facets at intermediate ΔK levels than the undeformed rail steel. At values near K_Q (the K value for fast failure under conditions that do not give a valid K_{IC}), the fracture surface contained mostly cleavage facets; the K_Q value for all the materials tested was 50 MPa$\sqrt{m}$.

The weld metal, however, exhibited mostly cleavage-faceted growth over the whole region of fatigue-crack growth. The size of the cleavage facets was 150 to 600 μm, and reflects the size of some structural parameter or parameters in the weld metal.

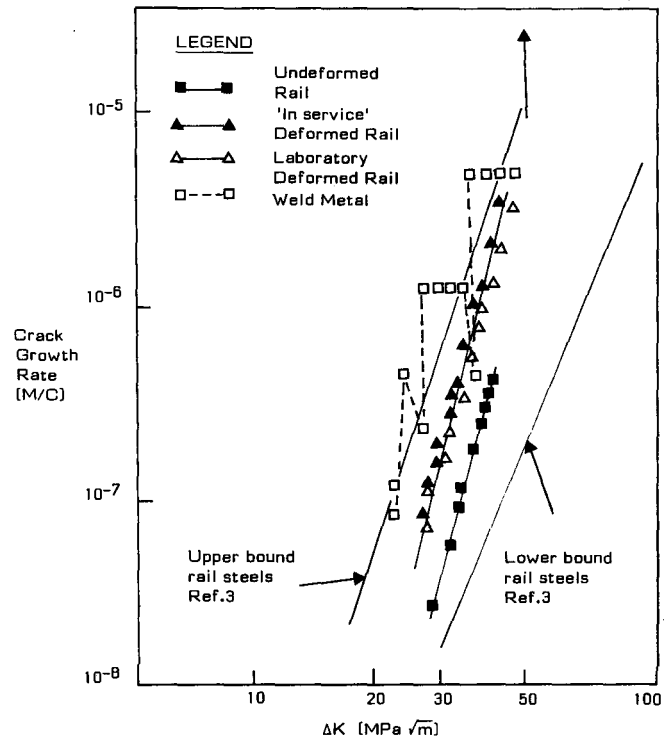

Fig. 1—Fatigue-crack growth (in metres per cycle) for deformed and undeformed rail steel and weld metal, compared with the upper and lower bounds of Hill and Bootle[3]

TABLE I
PARIS LAW EQUATIONS

Undeformed rail steel	$\frac{da}{dN}$ (m/c) = 1,92 × 10^{-7} $(\Delta K)^{6,3}$
Deformed rail steel	$\frac{da}{dN}$ (m/c) = 1,41 × 10^{-17} $(\Delta K)^{6,9}$
Weld metal	$\frac{da}{dN}$ (m/c) = 4,75 × 10^{-19} $(\Delta K)^{8,8}$
Upper bound of data on rail steel (after Steele[4])	$\frac{da}{dN}$ (m/c) = 2,68 × 10^{-15} $(\Delta K)^{5,56}$

m/c = metres per cycle

Discussion

From the results, it can be seen that plastic deformation ($\epsilon = 0,1$ per cent) slightly increased the crack growth in the rail steels by a factor of 2 to 3. The exponent n in the Paris Law equation obtained from the present study on rail steels indicated a value of 6 to 7, and this agrees well with the data of Evans *et al.*[5] and Steele[4] (Fig. 2).

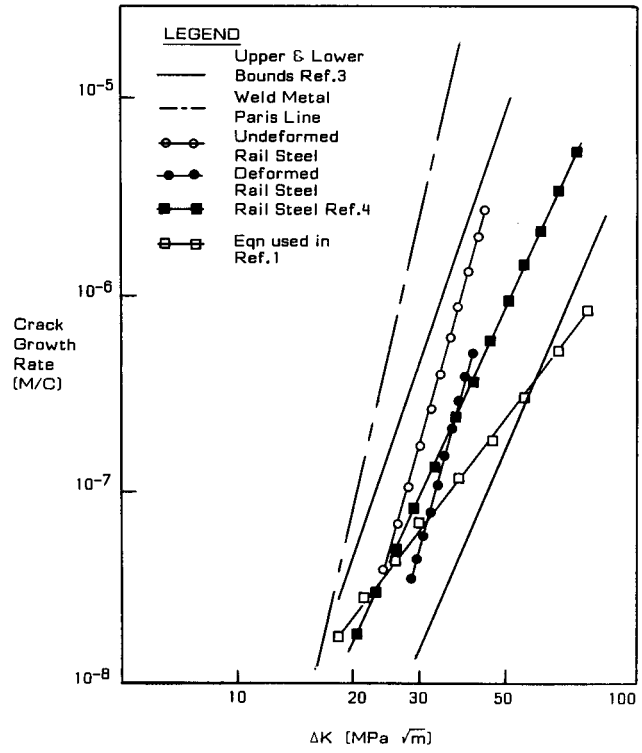

Fig. 2—Schematic diagram of fatigue-crack growth (in metres per cycle) for rail steels from various sources

The Paris Law equation for the weld metal exhibited an n value of approximately 9, which is common when static modes of fracture predominate. However, the equation used by Garrett and Tait[1] to assess the fatigue life of rail steel has an exponent of 2,5, which is about half the value typically found in rail-steel fatigue. Rapid local changes in the value of n were observed by Beevers *et al.*[6], which were the result of bursts of cleavage failure.

The L.E.F.M. approach to design against failure in structural materials involves basically a consideration of stress intensity in which criteria are established for fracture instability in the presence of a crack[7]. The essence of this approach is to relate the stress field developed in the crack vicinity to the applied normal stress on the material properties of a structure, and to the geometry and defect size necessary to initiate failure.

In the determination of the cyclic-life characteristics of a material, the first step is to identify the critical defect size for failure, a_{crit}. This is obtained by use of the pertinent expression for the stress intensity of a surface crack:

$$K_I^2 = \frac{1{,}21\ a\ \pi\sigma^2}{Q},$$

where K_I = nominal K, MPa$\sqrt{m}$
a = depth of surface crack, m
σ = applied stress, MPa
Q = parameter for flaw shape.

Rearrangement gives an expression for the critical flaw size:

$$a_{crit} = \frac{K^2_{crit}\ Q}{1{,}21\pi\ \sigma^2}.$$

For the present calculations, σ_{max} was taken[1] as 250 MPa. The σ/σ_{ys} is approximately 0,5, so that the Q values for the ratio of surface flaw length (a) to depth ($2c$) of 4:1 and 10:1 were 1,14 and 1,0 respectively. The K_{crit} values are taken from dynamic data on fracture toughness, K_{ID}, at 0°C. For rail steels, the value[1] of K_{ID} = 30 MPa$\sqrt{m}$, while the data for fully pearlitic steels indicate an extrapolated K_{ID} value of 17 to 20 MPa $\sqrt{m}$ for a coarse-grained pearlitic weld metal[8] (Fig. 3). K_{ID} data were used in the present case because of the likelihood of high strain-rate shock-loading conditions.

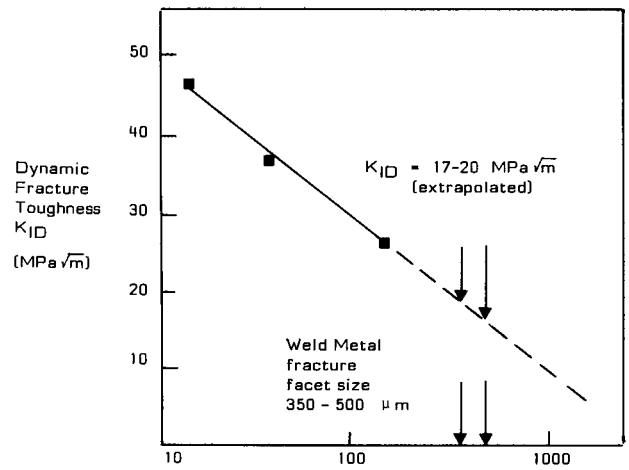

Fig. 3—Dynamic fracture toughness, K_{ID}, at 0°C for fully pearlitic steels as a function of austenite grain size[7]

The calculated values of a_{crit} for rail steels and weld metal for $a/2c$ = 4:1, were 5,3 mm and between 2,5 and 1,7 mm respectively. The corresponding values for $a/2c$ = 10:1 were 4,1 mm and between 1,3 and 1,7 mm.

When the present experimentally determined values are combined with the calculated values of a_{crit}, it is possible to compute the number of cycles required for an existing subcritical flaw to grow to failure. Wilson[9] has developed a generalized expression for cycle life:

$$N = \frac{2}{(n-2)C_o M^{n/2}(\Delta\sigma)^n}\left[\frac{1/n^{-2}}{a_1^1} - \frac{1/n^{-2}}{a_{crit}^{\ 2}}\right]$$

where N = number of cycles to failure
n = Paris exponent
C_o = Paris constant
a_1 = initial defect size
a_{crit} = critical defect size
$\Delta\sigma$ = stress range
M = parameter for flaw shape and geometry, which for surface defects is $1{,}21\pi/Q$.

It is assumed that the cyclic stress range, $\Delta\sigma$, is constant throughout the life of the component.

When the equation is solved for N at the $\Delta\sigma$ values (viz 155 and 104 MPa) and at a_1 values varying from 1 mm to the value of a_{crit}, curves of cyclic life can be drawn that relate the maximum initial allowable flaw size to the number of cycles required to cause failure at the appropriate $\Delta\sigma$.

The resulting curves of cyclic life for a ratio of flaw length to a depth of 4,1 are shown in Figs. 4 and 5, while

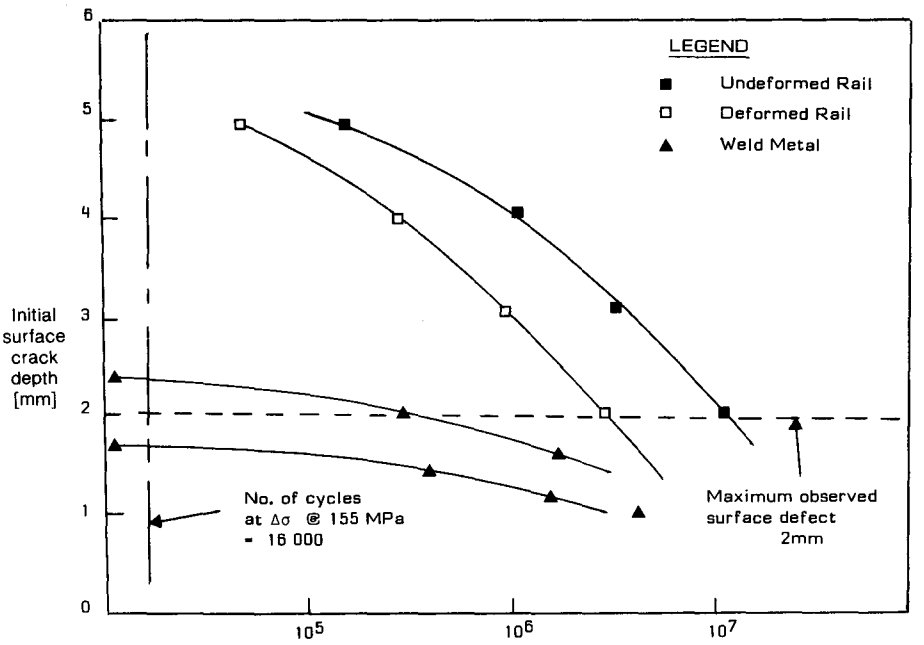

Fig. 4—Cyclic-life characteristics for $\Delta\sigma$ = 155 MPa, σ_{max} = 250 MPa, and ratio of surface-flaw length to depth = 4 : 1

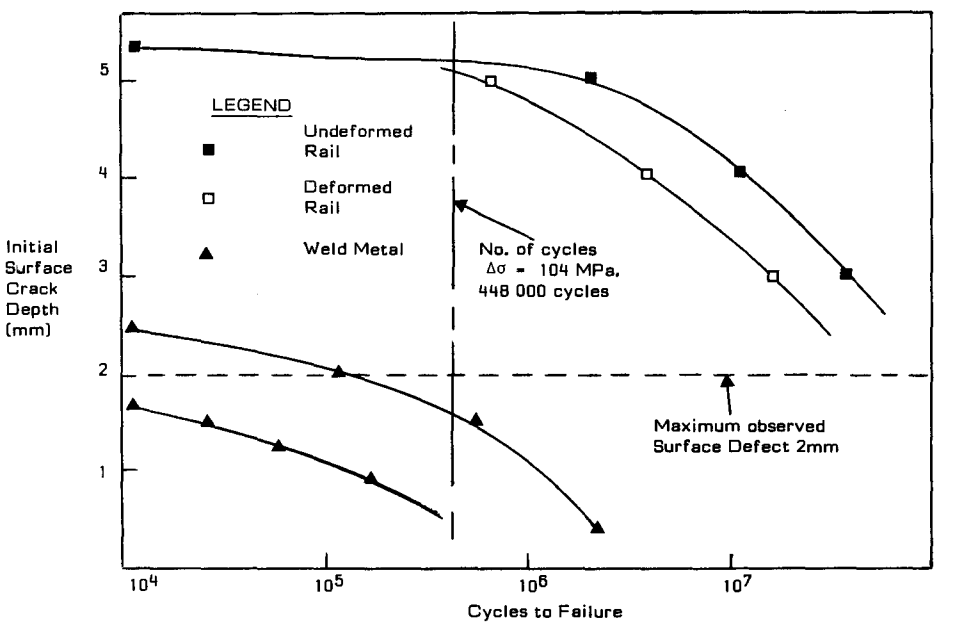

Fig. 5—Cyclic-life characteristics for $\Delta\sigma$ = 104 MPa, σ_{max} = 250 MPa, and ratio of surface-flaw length to depth = 4 : 1

those with a ratio of 10:1 are shown in Figs. 6 and 7.

These curves can be viewed or assessed in two ways:

(a) as the effect of a number of cycles on the value of a_{crit}, and

(b) as the number of cycles required to produce a_{crit} for a known initial flaw size in the material under assessment.

Thus, in the diagrams showing cyclic life, a vertical line was drawn to denote the number of cycles representing 8 years of service for a particular stress range (i.e. 16 000 at $\Delta\sigma$ = 155 MPa and 448 000 at $\Delta\sigma$ = 104 MPa) and a horizontal line representing the maximum defect size observed in rail steel material (in this case 2 mm).

What is immediately obvious from these diagrams is that both the deformed and the undeformed rail steel have cyclic lives that are far in excess of the number of service cycles at both levels of $\Delta\sigma$ and $a/2c$ ratios. For example, in Fig. 4 16 000 cycles at 155 MPa is far less than the number of cycles required to produce a critical flaw size of 2 mm. Indeed, for the deformed rail this number of cycles would have to be increased 170-fold, while the increase for the undeformed rail would be 625-fold, before failure could occur, i.e. before a_{crit} is attained. Just as striking as the immunity of the rail steels to fatigue failure over a service period of 8 years is the fact that, in all cases, the weld metal represents a problem in as much as fatigue failures were in some cases predicted within the period of its service life.

For a 4:1 ratio, the range in cyclic life lies above and below 2 mm and, as such, is bordering at Δ = 155 MPa, but predicts weld failures (a_i = 2 mm) at the $\Delta\sigma$ = 104

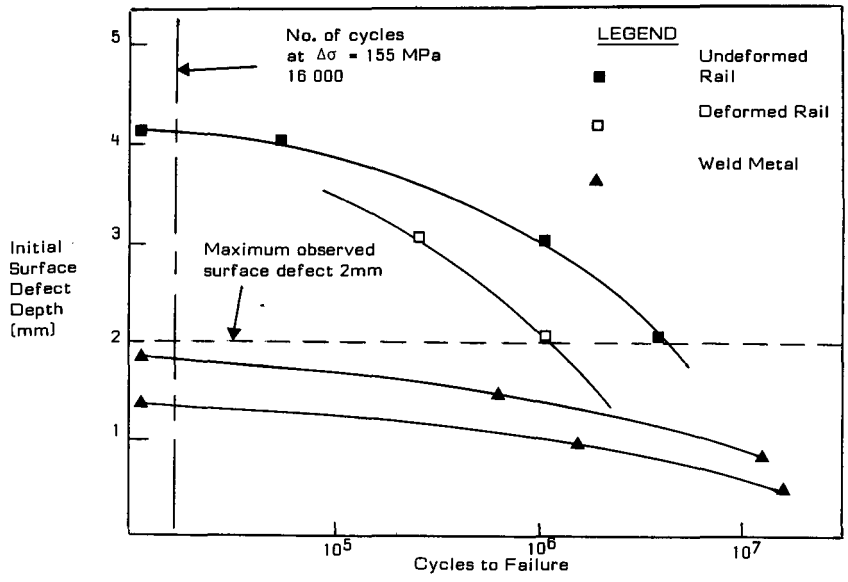

Fig. 6—Cyclic-life characteristics for $\Delta\sigma$ = 155 MPa, σ_{max} = 250 MPa, and ratio of surface-flaw length to depth = 10 : 1

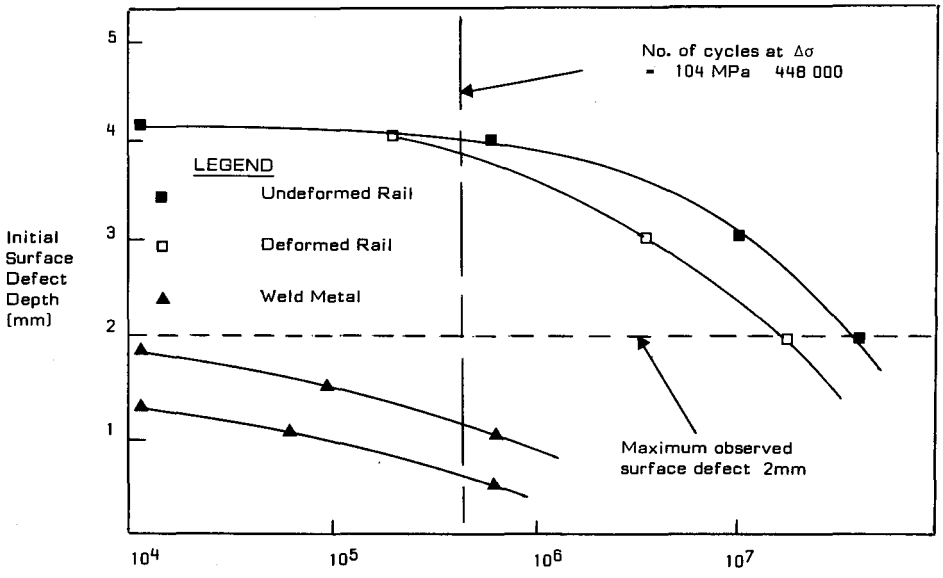

Fig. 7—Cyclic-life characteristics for $\Delta\sigma$ = 104 MPa, σ_{max} = 250 MPa, and ratio of surface-flaw length to depth = 10 : 1

MPa. The case of a 10:1 ratio predicts failures at both stress levels.

As failures of weld metals are potentially very serious, consideration must be given to the various input parameters at this point.

(1) *Dynamic Fracture Toughness*

The value of K_{ID} at 0°C that was ascribed to the weld metal, which had a fully pearlitic microstructure, was 17 to 20 MPa $\sqrt{m}$. These values represent extrapolated values of reported data on the effect of austenite grain size on K_{ID} in fully pearlitic structures. It is possible that the effect of grain size could indeed 'tail off' and that the K_{ID} values could be as high as 25 MPa$\sqrt{m}$ (Fig. 3). This would obviously affect a_{crit}.

(2) *Maximum Stress*

The estimated value of σ_{max} was taken from Garrett and Tait[1] and represents a 'worst case'. Again, if this is an over-estimation, the real a_{crit} will be higher.

(3) *Fatigue-crack Growth*

The Paris Law type of equation used for weld metal represents, at certain ΔK levels, a gross overestimation (in some cases, 5 times greater than the upper bound for rail steels), again portraying a somewhat pessimistic approach.

(4) *Initial Flaw Size*

This was taken as 2 mm, which represents the maximum lap-type defect that has been observed in rail steels. It would be interesting to know how many times such a defect has been encountered, and an actual size distribu-

tion of such surface defects in rail steels would prove invaluable in assessments of cyclic life.

(5) *Microstructure of the Weld Metal*

As only one weld metal was examined and tested in the present work, a number of selected welds in rail steel need to be studied to establish whether this particular weld metal is typical or not.

In view of the above limitations, it must be stated that the prediction of failure of the weld metal during service represents a compounded 'worst case' situation that could be ultra-conservative in nature. More reliable (experimentally determined) data are required before a justifiably realistic assessment can be achieved.

Conclusions

The work on the growth of fatigue cracks showed that

(a) the growth rates in the deformed rail steel were slightly higher than those in the undeformed rail steel, and
(b) the growth rates in the weld metal were appreciably faster and exhibited plateaux that were beyond the upper bound for rail steels.

Essentially, the cyclic-life curves show that no fatigue failures will occur during 8 years of service in both the deformed and the undeformed rail steels examined.

PART 2: METALLOGRAPHIC AND FRACTOGRAPHIC DETAILS

A section from the broken half of each fatigue fracture described in Part 1 was cut and cleaned electrolytically by use of the Endox-based technique. Each companion fracture surface was mounted in an electrically conducting medium so that the fatigue crack–microstructure profile could be studied. All the fractographic studies and most of the metallographic surveys were conducted on a Hitatchi 620 scanning electron microscope (SEM).

Measurements of the pearlite interlamellar spacing were taken for both the rail steels and the weld metal. For each microstructure, 100 random fields were taken, at a magnification of 2000 to 5000, and the number of lamellar intercepts was counted on a linear grid mounted on the screen of the SEM. The total length of line divided by the number of cementite lamellae intersected is defined as $\bar{\ell}$, the mean intercept spacing. The mean true pearlite spacing is given by $\lambda_0 = \bar{\ell}/2$. More exact forms of this equation have been developed for situations where not all the cementite platelets have a planar orientation, and details of the various methods available for the measurement of pearlite interlamellar spacing have been reported by Underwood[10].

Experimental Results

Microstructural Details

Microstructural details of the rail steel (the microstructures of the undeformed and deformed rail steel were almost identical) and of the weld metal are shown in Fig. 8. The rail steel exhibits a fine fully pearlitic microstructure, colony size approximately 50 μm, with little evidence of pro-eutectoid ferrite, while the weld metal shows extensive ferrite formation, which tends to decorate prior austenite grain boundaries. Much of the ferrite is nucleated along columnar grain boundaries (Fig. 8b) that were 0,5 to 1 mm in width. Again, the microstructure was predominantly pearlitic, and the pearlite colony was much coarser than that of the rail steel, measuring up to 300 μm in some instances. Mean measurements of true interlamellar pearlite spacing were recorded for each microstructure, with the following results: undeformed rail steel 184 nm, deformed rail steel 175 nm, and weld metal 136 nm.

Details of the nature of the pro-eutectoid ferrite formed in the weld metal are shown in Fig. 9: (a) illustrates the

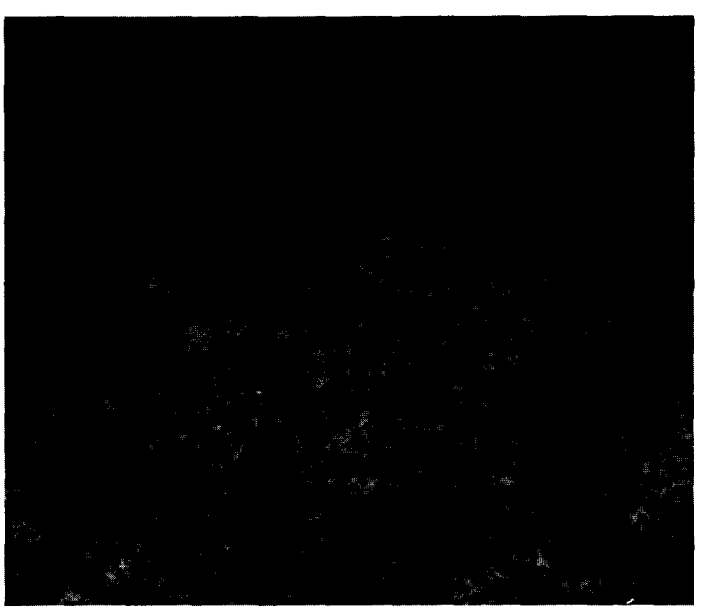

(a) General macrograph of undeformed rail steel, showing the relatively fine size of the pearlite colony and no evidence of grain-boundary polygonal ferrite

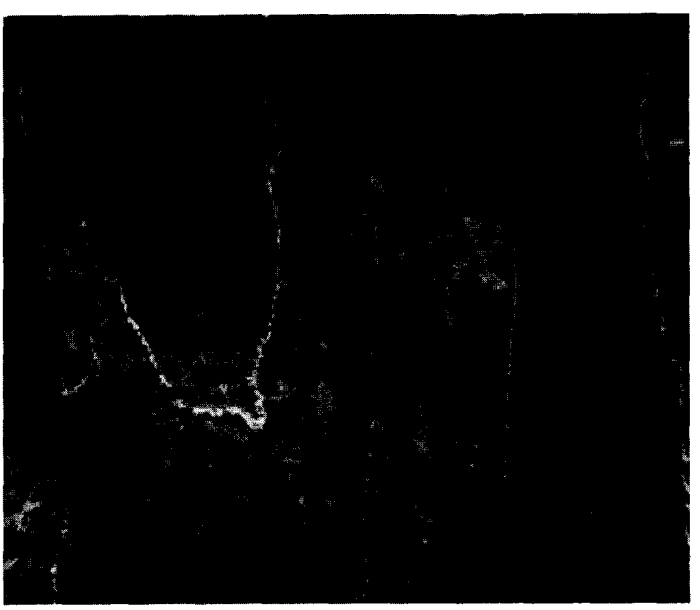

(b) General macrograph of the weld metal, showing large columnar grains decorated with polygonal ferrite, the grains varying in width from 0,5 to 1 mm; and showing the large size of the pearlite colony

Fig. 8—Microstructural details of the rail steel and the weld metal